JOURNAL OF PROPULSION AND POWER
Vol. 10, No. 4, July–Aug. 1994

Application of Dynamical Systems Theory to Nonlinear Combustion Instabilities

Craig C. Jahnke*
Clarkson University, Potsdam, New York 13699
and
F. E. C. Culick†
California Institute of Technology, Pasadena, California 91125

Two important approximations have been incorporated in much of the work with approximate analysis of unsteady motions in combustion chambers: 1) truncation of the series expansion to a finite number of modes, and 2) time-averaging. A major purpose of the present analysis is to investigate the limitations of those approximations. A continuation method is used to determine the limit cycle behavior of the time-dependent amplitudes of the longitudinal acoustic modes in a combustion chamber. The results show that time-averaging works well only when the system is slightly unstable. In addition, the stability boundaries predicted by the two-mode approximation are shown to be artifacts of the truncation of the system. Systems of two, four, and six modes are analyzed and show that more modes are needed to analyze more unstable systems. For the six-mode approximation with an unstable second-mode, two bifurcations are found to exist: 1) a pitchfork bifurcation leading to a new branch of limit cycles, and 2) a torus bifurcation leading to quasiperiodic motions.

I. Introduction

BECAUSE combustion instabilities arise normally as linearly unstable motions, nonlinear processes must be present to prevent the instabilities from growing without limit. Experimentally, therefore, nonlinear behavior is always observed. Serious analysis of nonlinear combustion instabilities began with work by Crocco,[1] Sirignano and Mitchell,[2] and Zinn[3,4] at Princeton in the 1960s. The results reported here are the most recent from a continuing investigation begun in the early 1970s, using a form of Galerkin's method.[5–7]

This approach is based on expressing any unsteady motion in a combustion chamber as a synthesis of normal modes

$$P' = \sum_{n=1}^{\infty} \eta_n(t)\psi_n(x), \qquad u' = a \sum_{n=1}^{\infty} \frac{\eta_n(t)}{\gamma k_n^2} \nabla\psi_n$$

where $\psi_n(x)$ are normal modes for the combustion chamber geometry in question. Spatial averaging converts the problem of solving the system of nonlinear partial differential equations to the much simpler problem of solving a system of nonlinearly coupled ordinary differential equations for the time-dependent amplitudes of the normal modes of the form

$$\ddot{\eta}_n + \omega_n^2 \eta_n = F_n$$

where F_n is a nonlinear function of η_n, $\dot{\eta}_n$, and time. Various tests have confirmed that accurate results can be obtained with this procedure for a broad range of conditions.[8] Hence, this system of equations, representing a collection of nonlinear oscillators, seems to be an acceptable formulation for studying various aspects of observed behavior understood poorly or not at all.

There are two main classes of nonlinear problems in this subject: 1) determining the conditions for existence and stability of limit cycles; and 2) determining the conditions under which a linearly stable system may become unstable when subjected to an appropriate disturbance. As a practical matter, two approximations have commonly been used to simplify the analysis and to try to obtain simpler methods for routine applications: 1) time-averaging converts the second-order equations to a first-order system governing the slowly changing amplitudes and phases of the modes; and 2) in any case the expansion must be truncated at a finite number of modes. It seems that the possible consequences and validity of those approximations can be understood only by solving the original system of second-order equations.

One approach is simply to compute numerical simulations for ranges of parameters characterizing the system. That tends to be a somewhat arbitrary approach. We choose here to apply some elementary notions of dynamical systems theory and construct bifurcation diagrams. Numerical simulations are then computed only for particularly interesting cases. We believe that this will provide a more systematic approach to understanding the matter cited above.

The equations analyzed in this article represent the time evolution of the amplitudes of the longitudinal acoustic modes in a combustion chamber of uniform cross section. Linear contributions from the combustion processes, gas/particle interactions, boundary conditions, and the interaction between the steady and unsteady flowfields are included along with nonlinear contributions from the gas dynamics. The equations representing the time evolution of the amplitudes of the longitudinal acoustic modes were obtained from Paparizos and Culick[9] and have the form

$$\ddot{\eta}_n + \omega_n^2\eta_n = 2\alpha_n\dot{\eta}_n + 2\theta_n\omega_n\eta_n - \sum_{i=1}^{n-1} [C_{ni}^{(1)}\dot{\eta}_n\dot{\eta}_{n-i} + D_{ni}^{(1)}\eta_i\eta_{n-i}] - 2\sum_{i=1}^{\infty} [C_{ni}^{(2)}\dot{\eta}_n\dot{\eta}_{n+i} + D_{ni}^{(2)}\eta_i\eta_{n+i}] \quad (1)$$

Presented as Paper 93-0114 at the AIAA 31st Aerospace Sciences Meeting and Exhibit, Reno, NV, Jan. 11–14, 1993; received Aug. 5, 1993; revision received Nov. 4, 1993; accepted for publication Nov. 19, 1993.

*Assistant Professor of Mechanical and Aeronautical Engineering. Member AIAA.
†Professor of Jet Propulsion and Mechanical Engineering. Fellow AIAA.

Table 1 First-mode instability

$\omega_1 = 5654.87$		
n	α_n, s^{-1}	θ_n, rad/s
1	$0 \rightarrow 300$	12.9
2	−324.8	46.8
3	−583.6	−29.3
4	−889.4	−131.0
5	−1262.7	−280.0
6	−1607.6	0.0

Table 2 Second-mode instability

$\omega_1 = 2827.435$		
n	α_n, s^{-1}	θ_n, rad/s
1	−84.9	−66.7
2	$0 \rightarrow 300$	12.9
3	−161.0	108.2
4	−279.4	46.8
5	−392.7	8.8
6	−520.2	−29.3

where

$$C_{ni}^{(1)} = \frac{-1}{2\gamma i(n-i)}[n^2 + i(n-i)(\gamma-1)]$$

$$C_{ni}^{(2)} = \frac{1}{2\gamma i(n+i)}[n^2 - i(n+i)(\gamma-1)]$$

$$D_{ni}^{(1)} = \frac{(\gamma-1)\omega_1^2}{4\gamma}[n^2 - 2i(n-i)]$$

$$D_{ni}^{(2)} = \frac{(\gamma-1)\omega_1^2}{4\gamma}[n^2 + 2i(n+i)]$$

This system of equations has the form of a system of nonlinearly coupled oscillators. The parameters α_n and θ_n account for the linear processes mentioned above and represent the linear damping and frequency shift of each mode, respectively. Parameter values used in this study were obtained from Paparizos and Culick[9] and are listed in Tables 1 and 2.

Since this study is restricted to longitudinal acoustic modes in a combustion chamber of uniform cross section, the modal frequencies are related by the relation $\omega_n = n\omega_1$. Substituting this relation into Eq. (1) and nondimensionalizing time with the fundamental acoustic frequency ($\hat{t} = \omega_1 t$, where $\hat{t}$ is nondimensional time) results in the system

$$\ddot{\eta}_n + n^2\eta_n = 2\hat{\alpha}_n\dot{\eta}_n + 2_n\hat{\theta}_n\eta_n - \sum_{i=1}^{n-1}\left[C_{ni}^{(1)}\dot{\eta}_n\dot{\eta}_{n-i} + \frac{1}{\omega_1^2}D_{ni}^{(1)}\eta_i\eta_{n-i}\right] - 2\sum_{i=1}^{\infty}\left[C_{ni}^{(2)}\dot{\eta}_n\dot{\eta}_{n+i} + \frac{1}{\omega_1^2}D_{ni}^{(2)}\eta_i\eta_{n+i}\right] \quad (2)$$

where

$$\hat{\alpha}_n = (\alpha_n/\omega_1) \qquad \hat{\theta}_n = (\theta_n/\omega_1)$$

To analyze Eq. (2) with techniques from dynamical systems theory and continuation methods it must be written as a first-order system. This can be done by defining the new variable

$$\xi_n = \dot{\eta}_n \quad (3)$$

The system then has the form

$$\dot{\eta}_n = \xi_n$$

$$\dot{\xi}_n = -n(n - 2\hat{\theta}_n)\eta_n + 2\hat{\alpha}_n\xi_n - \sum_{i=1}^{n-1}[\hat{C}_{ni}^{(1)}\xi_i\xi_{n-i} + \hat{D}_{ni}^{(1)}\eta_i\eta_{n-i}] - \sum_{i=1}^{\infty}[\hat{C}_{ni}^{(2)}\xi_i\xi_{n+i} + \hat{D}_{ni}^{(2)}\eta_i\eta_{n+i}] \quad (4)$$

where

$$\hat{C}_{ni}^{(1)} = \frac{-1}{2\gamma i(n-i)}[n^2 + i(n-i)(\gamma-1)]$$

$$\hat{C}_{ni}^{(2)} = \frac{1}{\gamma i(n+i)}[n^2 - i(n+i)(\gamma-1)]$$

$$\hat{D}_{ni}^{(1)} = \frac{\gamma-1}{4\gamma}[n^2 - 2i(n-i)]$$

$$\hat{D}_{ni}^{(2)} = \frac{\gamma-1}{2\gamma}[n^2 + 2i(n+i)]$$

Time-averaging is applied to Eq. (4) by assuming that the time-dependent amplitude of each acoustic mode has the form

$$\eta_n(\hat{t}) = A_n(\hat{t})\sin(n\hat{t}) + B_n(\hat{t})\cos(n\hat{t}) \quad (5)$$

Substituting Eq. (5) into Eq. (4) and averaging the resulting system over the period ($0 \rightarrow 2\pi$) results in the system[9]

$$\dot{A}_n = \hat{\alpha}_n A_n + \hat{\theta}_n B_n + \frac{1}{2}n\kappa\sum_{i=1}^{n-1}(A_iA_{n-i} - B_iB_{n-i}) - n\kappa\sum_{i=1}^{\infty}(A_{n+i}A_i + B_{n+i}B_i)$$

$$\dot{B}_n = \hat{\alpha}_n B_n - \hat{\theta}_n A_n + \frac{1}{2}n\kappa\sum_{i=1}^{n-1}(A_iB_{n-i} + B_iA_{n-i}) - n\kappa\sum_{i=1}^{\infty}(A_{n+i}B_i - B_{n+i}A_i) \quad (6)$$

where

$$\kappa = (\gamma+1)/8\gamma$$

Steady states of Eq. (6) represent limit cycles of the time-dependent amplitudes of the acoustic modes η_n, due to the time dependence specified by Eq. (5).

The zero solution of Eq. (6) ($A_n = B_n = 0$) represents a zero pressure perturbation of the original system. The stability of this steady state is given by the eigenvalues of the linearized system

$$\lambda_n = \hat{\alpha}_n \pm i\hat{\theta}_n$$

Thus, when α_n is zero, this system undergoes a Hopf bifurcation. Hopf bifurcations lead to the existence of limit cycles, so when α_n is positive, Eq. (6) will undergo limit cycle behavior. This seems to suggest that time-averaging did not make the continuation problem any easier because the time-averaged system also contains limit cycles. Thus, when applying the continuation method to the time-averaged system it is necessary to continue a limit cycle as opposed to a steady state. This is an important distinction because the computer time required to determine the limit cycles of a system with

continuation methods is several orders of magnitude longer than the computer time required to determine the steady states of the system. Time-averaging does reduce the computational time required to do numerical simulations as the high-frequency content of the pressure fluctuation is eliminated by time-averaging, making it possible to use larger time steps in the simulation.

Applying time-averaging to Eq. (4) did not convert the limit cycles of Eq. (4) to steady states of Eq. (6), because the van der Pol transformation applied before time-averaging [Eq. (5)] did not use the proper frequency in the sine and cosine terms. The eigenvalues of the system obtained by linearizing Eq. (4) about the origin are

$$\lambda_n = \hat{\alpha}_n \pm in\sqrt{1 - (2\hat{\theta}_n/n) - (\hat{\alpha}_n/n)^2} = \hat{\alpha}_n \pm i\Omega_n$$

and so the van der Pol transformation should have the form

$$\eta_n(\hat{t}) = A_n(\hat{t})\sin(\Omega_n\hat{t}) + B_n(\hat{t})\cos(\Omega_n\hat{t}) \tag{7}$$

It is not possible to apply time averaging with this van der Pol transformation as the frequencies Ω_n are not integer multiples of each other. A limit cycle of a given frequency will exist for the complete system through the interaction of the nonlinear terms, but it is not possible to calculate this frequency analytically.

Since Eq. (6) is expected to contain limit cycles as asymptotic motions it is useful to transform Eq. (6) into polar coordinates. Applying the coordinate transformation

$$A_n = r_n \cos\phi_n$$

$$B_n = r_n \sin\phi_n \tag{8}$$

to Eq. (6) results in the system

$$\dot{r}_n = \hat{\alpha}_n r_n + \frac{1}{2} n\kappa \sum_{i=1}^{n-1} r_i r_{n-i} \cos(\phi_i + \phi_{n-i} - \phi_n) - n\kappa \sum_{i=1}^{\infty} r_i r_{n+i} \cos(\phi_i - \phi_{n+i} + \phi_n)$$

$$\dot{\phi}_n = \hat{\theta}_n + \frac{1}{2} n\kappa \sum_{i=1}^{n-1} \left(\frac{r_i r_{n-i}}{r_n}\right) \sin(\phi_i + \phi_{n-i} - \phi_n) + n\kappa \sum_{i=1}^{\infty} \left(\frac{r_i r_{n+i}}{r_n}\right) \sin(\phi_i - \phi_{n+i} + \phi_n) \tag{9}$$

Paparizos and Culick[9] have shown that in the limit cycle one would expect the frequencies of the time-dependent amplitudes of the acoustic modes $[\omega_n - n\dot{\phi}_n(\hat{t})]$ to be integer multiples of each other. Since $\omega_n = n\omega_1$ for the case considered here, one might expect

$$\frac{d}{dt}[\phi_n(t) - n\phi_1(t)] = 0$$

in the limit cycle. With this in mind it seems useful to replace the variables ϕ_n by the new variables $\psi_n = n\phi_1 - \phi_n$. Substituting this new variable into Eq. (9) results in the system

$$\dot{r}_n = \hat{\alpha}_n r_n + \frac{1}{2} n\kappa \sum_{i=1}^{n-1} r_i r_{n-i} \cos(\psi_n - \psi_{n-i} - \phi_i) - n\kappa \sum_{i=1}^{\infty} r_i r_{n+i} \cos(\psi_{n+i} - \psi_n - \psi_i)$$

$$n = 1, \ldots, N$$

$$\dot{\psi}_n = (\hat{\theta}_n - n\hat{\theta}_1) - \frac{1}{2} n\kappa \sum_{i=1}^{n-1} \left(\frac{r_i r_{n-i}}{r_n}\right) \sin(\psi_n - \psi_{n-i} - \psi_i) + n\kappa \sum_{i=1}^{\infty} \left(\frac{r_i r_{n+i}}{r_n}\right) \sin(\psi_{n+i} - \psi_n - \psi_i) + n\kappa \sum_{i=1}^{\infty} \left(\frac{r_i r_{i+1}}{r_1}\right) \sin(\psi_{i+1} - \psi_i)$$

$$n = 2, \ldots, N \tag{10}$$

Note that ψ_1 is zero by definition, so the dimension of the system is reduced from $2N$ to $2N - 1$. This reduction in the order of the system is possible because the reference value of the phase is arbitrary; the important quantity is the difference between the phases of the various modes. Thus, one can define all phases relative to the phase of the fundamental mode as was done above.

II. Theoretical Background

A. Dynamical Systems Theory

Dynamical systems theory is a methodology for studying systems of ordinary differential equations. Many systems have been studied using dynamical systems theory, but it has not been used to study nonlinear acoustics in combustion chambers. The important ideas of dynamical systems theory used in this report will be introduced in the following paragraphs. More information can be found in the book of Guckenheimer and Holmes.[10]

The first step in analyzing a system of nonlinear differential equations, in the dynamical systems theory approach, is to calculate the steady states of the system and their stability. Steady states can be determined by setting all time derivatives equal to zero and solving the resulting set of algebraic equations. The Hartman-Grobman Theorem (Ref. 10, Chap. 1, p. 13) proves that the local stability of a steady state can be determined by linearizing the equations of motion about the steady state and calculating the eigenvalues. A steady state is linearly stable if the real parts of the eigenvalues are negative and linearly unstable if any eigenvalue has a positive real part. In the neighborhood of a steady state (i.e., a region where the linear analysis is valid) the system will be attracted to the steady state if it is stable and repelled from the steady state if it is unstable.

The Implicit Function Theorem (Ref. 11, Chap. 2, pp. 13, 14) proves that the steady states of a system are continuous functions of the parameters of the system. Thus, the steady states of the nonlinear acoustic equations are continuous functions of the linear stability parameters of each mode α_n. Stability changes can occur as the parameters of the system are varied in such a way that the real parts of one or more eigenvalues of the linearized system change sign. Changes in the stability of a steady state lead to qualitatively different responses for the system and are called bifurcations. Stability boundaries can be determined by searching for steady states which have one or more eigenvalues with zero real parts.

There are many types of bifurcations and each type has a different effect on the response of the system. Qualitative changes in the response of the system can be predicted by determining how many and what type of eigenvalues have zero real parts at the bifurcation point. Bifurcations for which one real eigenvalue is zero lead to the creation or destruction of two or more steady states. Bifurcations for which one pair of imaginary eigenvalues has zero real parts can lead to the creation or destruction of periodic motions. Bifurcations for which more than one real eigenvalue or more than one pair of imaginary eigenvalues have zero real parts lead to very complicated behavior and are beyond the scope of this report.

Results presented in this report will also be concerned with the limit cycle behavior of dynamical systems. In particular, the pressure oscillations referred to as combustion instabilities in combustion systems are represented by limit cycles of the amplitude equations. Limit cycles can undergo bifurcations analogous to the bifurcations of steady states discussed above. Analytical results generally involve the study of the Poincare map of the system. Bifurcations of limit cycles occur when one or more eigenvalues of the linearized map about the limit cycle have magnitude equal to 1. One real eigenvalue equal to $+1$ signifies a pitchfork bifurcation, one real eigenvalue equal to -1 signifies a period doubling bifurcation, and one pair of imaginary eigenvalues with magnitude 1 signifies a Hopf bifurcation of the limit cycle, commonly called a torus

bifurcation. A thorough discussion of the various types of bifurcations of both steady states and limit cycles is given in Guckenheimer and Holmes.[10]

B. Continuation of Steady States

Continuation methods are a direct result of the Implicit Function Theorem, which proves that the steady states of a system are continuous functions of the parameters of the system. The general technique is to fix all parameters of the system but one, and compute the steady states of the system as a function of this parameter. For a system of ordinary differential equations of the form

$$\dot{x} = f(x, \mu) \tag{11}$$

where x is a vector representing the state of the system, and μ is a one-dimensional parameter, the implicit function theorem proves that the steady states of the system are continuous functions of the parameter μ. Thus, solutions of the equation

$$f(x, \mu) = 0 \tag{12}$$

are continuous functions of μ. Continuation methods are numerical techniques for calculating solutions of Eq. (12).

The technique used in this work is called a pseudo-arc-length continuation technique and is from Doedel and Kernevez.[12] In this numerical technique the parameter μ is treated as an unknown along with x, and steady states are calculated as functions of the arc length s along the curve of steady states. If one steady state of the system is known, a new steady state can be approximated by linear extrapolation from the know steady state as shown in Fig. 1. The slope of the curve at the known steady state can be determined by taking the derivative of Eq. (12) with respect to s

$$f_x x' + f_\mu \mu' = 0 \tag{13}$$

where

$$x' = \frac{dx}{ds} \qquad \mu' = \frac{d\mu}{ds} \tag{14}$$

and solving for x' and μ'. The change of x and μ in one step along the curve is limited by normalizing x' and μ' with the relation

$$(x')^2 + (\mu')^2 = 1 \tag{15}$$

The error between the approximate steady state and the true steady state is then reduced to an acceptable level with Newton's method.

The above technique is computationally expensive as it requires the matrix (f_x, f_μ) to be inverted to solve for x' and μ' at each step. If two steady states of Eq. (11), (x_0, μ_0) and (x_1, μ_1), are known, an approximation to the above technique can be used. This involves approximating Eq. (15) with the pseudo-arc-length continuation equation of Keller[13]

$$(x - x_1)x_1' + (\mu - \mu_1)\mu_1' - \Delta s = 0 \tag{16}$$

where Δs is the step size along the solution curve, and x_1' and μ_1' are the values of x' and μ' evaluated at (x_1, μ_1). The values of x_1' and μ_1' are approximated by (see Fig. 2)

$$x_1' = \frac{(x_1 - x_0)}{\Delta s}, \qquad \mu_1' = \frac{(\mu_1 - \mu_0)}{\Delta s} \tag{17}$$

Steady states of Eq. (11) are calculated by solving

$$f(x, \mu) = 0$$
$$(x - x_1)x_1' + (\mu - \mu_1)\mu_1' - \Delta s = 0 \tag{18}$$

with the following algorithm: 1) approximate x_1' and μ_1' at the known steady state; 2) approximate the unknown steady state, $x = x_1 + x_1'\Delta s$, $\mu = \mu_1 + \mu_1'\Delta s$; and 3) use Newton's method to reduce the error between the approximate and true steady state to an acceptable level.

C. Continuation of Limit Cycles

To study combustion instabilities it is also necessary to compute the limit cycles of a dynamical system. It is possible to compute the limit cycles of a dynamical system by discretizing the system in time to turn the computation of limit cycles into a continuation of steady states. More specifically, periodic orbits of Eq. (11) are given by solutions of

$$\dot{x} - \tau f[x(t), \mu] = 0$$
$$x(0) - x(1) = 0 \tag{19}$$

where τ is the period of the limit cycle and time has been scaled by the relation $t \rightarrow t/\tau$. Using the techniques discussed above for steady states, μ will be treated as an unknown and solutions will be calculated as functions of arc length s along the curve of limit cycles. Since the period of the limit cycle τ is unknown, another equation is needed to make the system solvable. The extra equation can be derived by noting that two periodic orbits at subsequent values of arc length have an arbitrary phase difference. This is true because if $x(t)$ is a limit cycle satisfying Eq. (19), then $x(t + \sigma)$ is also a limit cycle satisfying Eq. (19). Thus, if $x_k(t)$ is a known periodic orbit, and $x(t)$ is the subsequent unknown periodic orbit, the arbitrary phase difference between the periodic orbits can be eliminated by minimizing[12]

$$g(\sigma) = \int_0^1 \|x(t + \sigma) - x_k(t)\|_2^2 dt \tag{20}$$

Equating the derivative of Eq. (20) to zero and integrating by parts gives the phase relation[12]

$$\int_0^1 \dot{x}(t)\dot{x}_k(t)\, dt = 0 \tag{21}$$

which will be used in the continuation technique.

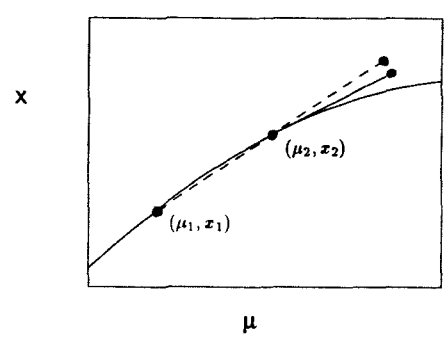

Fig. 1 Graphical representation of continuation method.

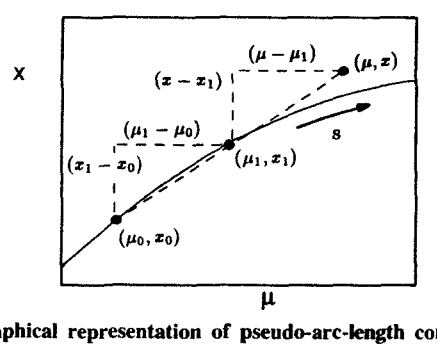

Fig. 2 Graphical representation of pseudo-arc-length continuation equation.

The pseudo-arc-length continuation equation used for calculating the steady states of a dynamical system, Eq. (16), can be generalized to calculate the limit cycles of a dynamical system. Time dependence of the solution can be accounted for by calculating the quantities represented by Eq. (16) over one period of the limit cycle[12]

$$\int_0^1 [x(t) - x_k(t)]x_k'(t)\,dt + (\mu - \mu_k)\mu_k' + (\tau - \tau_k)\tau_k' - \Delta s = 0 \tag{22}$$

The complete system for calculating the $(k+1)^{st}$ limit cycle of Eq. (11) when the kth limit cycle is known is

$$F[x(t);\,\mu,\,\tau] = \begin{Bmatrix} \dot{x} - \tau f[x(t),\,\mu] \\ x(0) - x(1) \\ \int_0^1 x(t)\dot{x}(t)\,dt \\ \int_0^1 [x(t) - x_k(t)]x_k'(t)\,dt \\ +\,(\mu - \mu_k)\mu_k' + (\tau - \tau_k)\tau_k' - \Delta s \end{Bmatrix} = 0 \tag{23}$$

It is exceedingly difficult, if not impossible, to analytically or computationally determine the functions $x(t)$ that satisfy these equations. One way of solving this system is to discretize the periodic orbit $x(t)$ in time. The particular technique of Doedel and Kernevez[12] is to divide the period $0 \le t \le 1$, into N intervals. In the jth interval define the Lagrange basis polynomial

$$a_{j,i}(t) = \prod_{k=0,k\neq i}^{m} \frac{t - [t_j + (k/m)\Delta t]}{[(i-k)/m]\Delta t} \tag{24}$$

and approximate the periodic orbit $x(t)$ in the jth interval by

$$x_j(t) = \sum_{i=0}^{m} a_{j,i}(t)u_{j+i/m} \tag{25}$$

The key characteristic of the basis polynomials is that

$$a_{j,i}[t_j + (i/m)\Delta t] = 1$$
$$a_{j,i}[t_j + (k/m)\Delta t] = 0, \qquad k \neq i \tag{26}$$

Thus

$$x_j[t_j + (i/m)\Delta t] = u_{j+i/m} \tag{27}$$

and $u_{j+i/m}$ represents the discrete approximation of the periodic solution $x(t)$, at time $t = t_j + (i/m)\,\Delta t$.

The method then consists of solving

$$\dot{x}_j(z_{j,i}) - \tau f[x_j(z_{j,i}),\ \mu] = 0 \tag{28}$$

for $i = 1, \ldots, m$ and $j = 1, \ldots, N$, where $z_{j,i}$ are the zeroes of the mth degree Legendre polynomial relative to the appropriate subinterval. This technique is a generalization of relaxation methods (Ref. 14, p. 609), in which ordinary differential equations are approximated by finite difference equations on a grid or mesh over the domain. The integral equations in Eq. (23) are discretized by a composite quadrature formula obtained by approximate integration over each subinterval of time (Ref. 14, p. 131). Gauss-Legendre quadratures are used in this work with $z_{j,i}$ as the collocation points.

The problem is then one of finding the steady states of a system of ordinary differential equations where the new variables are the $u_{j+i/m}$. This is much easier than finding the periodic orbits of Eq. (11), and one that can be solved with the continuation algorithm discussed above, but this simplification comes at a price. Discretizing the system results in a large increase in the dimension of the system to be solved. If the dimension of the original system, Eq. (11), is n, and the system is discretized into N time intervals with m collocation points in each subinterval, then the dimension of the discretized system will then be $Nmn + n + 2$.

The stability of the periodic orbits is determined by calculating the Floquet multipliers of the discretized system (Ref. 10, p. 24). Floquet multipliers of a periodic orbit are analogous to the eigenvalues of a steady state. In the present work, an approximation to the linearized Poincare map is used to calculate the Floquet multipliers of the periodic orbit (Ref. 12, p. 44). Bifurcations can be found by searching for periodic orbits that have one or more Floquet multipliers whose magnitude is one.

III. Analysis of Steady States

The steady states of Eq. (4) are determined by setting the time derivatives equal to zero ($\dot{\eta}_n = \dot{\xi}_n = 0$) and solving the resulting algebraic equations. It is easy to see that the zero solution, $(\eta_n, \xi_n) = (0, 0)$, is a steady state for Eq. (4), no matter how many modes are included in the system. This steady state corresponds to zero pressure perturbation in the combustion chamber.

The stability of the zero steady state can be determined by calculating the eigenvalues of the system obtained by linearizing Equation (4) about the origin. Linearizing Eq. (4) about the origin gives

$$\begin{pmatrix} \dot{\eta}_n \\ \dot{\xi}_n \end{pmatrix} = \begin{bmatrix} 0 & 1 \\ -(n^2 - 2n\hat{\theta}_n) & 2\hat{\alpha}_n \end{bmatrix} \begin{pmatrix} \eta_n \\ \xi_n \end{pmatrix} \tag{29}$$

Note that the acoustic modes represented by Eq. (4) are linearly uncoupled, so the linearized system for an N-mode approximation will consist of N pairs of linear, uncoupled equations. Therefore, it is possible to determine the eigenvalues of the linearized system independent of the number of modes included in the truncated system. The eigenvalues of the nth mode are

$$\lambda_n = \hat{\alpha}_n \pm in\sqrt{1 - (2\hat{\theta}_n/n) - (\hat{\alpha}_n/n)^2} \tag{30}$$

If $\hat{\alpha}_n$ is zero, then the eigenvalues of the nth mode are pure imaginary and a Hopf bifurcation occurs. This leads to the existence of limit cycles when $\hat{\alpha}_n$ is positive for one or more modes. These limit cycles represent time varying amplitudes of the acoustic modes and are physically realized as combustion instabilities.

Jahnke[15] has shown that Eq. (4) has steady states besides the steady state at the origin. A pair of nonzero steady states can be determined analytically for the two-mode approximation, but they are physically unrealistic as they are greater than one. In particular, for $\gamma = 1.4$, the steady states are given by $(\eta_1, \eta_2) = (\pm 6.3, 1.4)$. These steady states are unstable so they will not affect the dynamics of the system near the origin.

Steady states other than the zero steady state were also found for the four- and six-mode approximations. These steady states were found using a continuation algorithm because it was impossible to determine the steady states analytically. Four nonzero steady states were found for the four-mode approximation. All these steady states were physically unrealistic and linearly unstable, and so they will not affect the dynamics of the system near the origin. Six nonzero steady states were found for the six-mode approximation; these were also physically unrealistic and linearly unstable.

IV. Results for a First-Mode Instability

A. Two-Mode Time-Averaged Results

The two-mode time-averaged equations in polar coordinates can be obtained from Eq. (10) to give the system of first-order ordinary differential equations

$$\dot{r}_1 = \hat{\alpha}_1 r_1 - \kappa r_1 r_2 \cos\psi_2$$

$$\dot{r}_2 = \hat{\alpha}_2 r_2 + \kappa r_1^2 \cos\psi_2$$

$$\dot{\psi}_2 = (\hat{\theta}_2 - 2\hat{\theta}_1) + \kappa[2r_2 - (r_1^2/r_2)]\sin\psi_2 \qquad (31)$$

Paparizos and Culick[9] derived an equivalent form of the two-mode time-averaged equations and went on to show that stable steady states of the two-mode time-averaged equations exist only if $\hat{\alpha}_2/\hat{\alpha}_1 < -2$ and that the steady states are given by

$$r_1 = (1/\kappa)\sqrt{-\hat{\alpha}_1\hat{\alpha}_2(1+\beta^2)}$$

$$r_2 = (1/\kappa)\sqrt{-\hat{\alpha}_1^2(1+\beta^2)}$$

$$\psi_2 = \tan^{-1}(-\beta) \qquad (32)$$

where

$$\beta = \frac{\hat{\theta}_2 - 2\hat{\theta}_1}{2\hat{\alpha}_1 + \hat{\alpha}_2}$$

It is important to note that the steady state of Eq. (31) does not necessarily represent a steady state of the two-mode time-averaged equations. The condition that $\dot{\psi}_2$ equals zero means that $2\dot{\phi}_1 - \dot{\phi}_2$ equals zero, but not necessarily that $\dot{\phi}_1$ and $\dot{\phi}_2$ are individually equal to zero. Using the steady-state values of r_1 and r_2 it is easy to show that

$$\dot{\phi}_1 = -\left(\frac{\hat{\alpha}_1\hat{\theta}_2 + \hat{\alpha}_2\hat{\theta}_1}{2\hat{\alpha}_1 + \hat{\alpha}_2}\right)$$

$$\dot{\phi}_2 = -2\left(\frac{\hat{\alpha}_1\hat{\theta}_2 + \hat{\alpha}_2\hat{\theta}_1}{2\hat{\alpha}_1 + \hat{\alpha}_2}\right) \qquad (33)$$

so the steady states of Eq. (31) represent limit cycles of the two-mode time-averaged equations. The solution of the two-mode time-averaged approximation to the nonlinear longitudinal acoustics in a combustion chamber is thus given by

$$n_1(t) = \frac{8\gamma}{(\gamma+1)\omega_1}\sqrt{-\alpha_1\alpha_2(1+\beta^2)}\sin[\omega_1 t + \phi_1(t)]$$

$$n_2(t) = \frac{8\gamma}{(\gamma+1)\omega_1}\sqrt{-\alpha_1^2(1+\beta^2)}\sin[2\omega_1 t + \phi_2(t)] \qquad (34)$$

where

$$\phi_1(t) = -\left(\frac{\alpha_1\theta_2 + \alpha_2\theta_1}{2\alpha_1 + \alpha_2}\right)t + \phi_{10}$$

$$\phi_2(t) = -2\left(\frac{\alpha_1\theta_2 + \alpha_2\theta_1}{2\alpha_1 + \alpha_2}\right)t + \phi_{20}$$

$$\beta = \left(\frac{\theta_2 - 2\theta_1}{2\alpha_1 + \alpha_2}\right)$$

$$2\phi_{10} - \phi_{20} = \tan^{-1}(-\beta)$$

Note that the time dependence of ϕ_1 and ϕ_2 changes the frequency of the limit cycle.

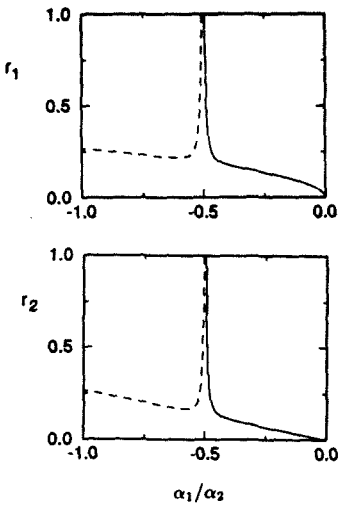

Fig. 3 Maximum amplitude of acoustic modes in limit cycle for two-mode time-averaged approximation; —— stable, --- unstable.

The maximum amplitudes of $\eta_1(t)$ and $\eta_2(t)$ in the limit cycle are shown in Fig. 3 as functions of α_1/α_2. Figure 3 shows that a limit cycle exists when α_1/α_2 is negative, but is stable only if α_1/α_2 is less than $-\frac{1}{2}$. It is important to note that the amplitude of the limit cycle goes to infinity as α_1/α_2 approaches $-\frac{1}{2}$, which coincides with the stability boundary of the limit cycle. Since the original equations representing the time evolution of the amplitudes of the acoustic modes were derived using a perturbation analysis, only limit cycles with small amplitudes are valid approximations to solutions of the complete fluid dynamic equations. Also, time-averaging is theoretically valid only if the amplitudes in the limit cycle remain small. Thus, one would expect that the limit cycles predicted by the two-mode time-averaged equations are not valid for values of α_1/α_2 near $-\frac{1}{2}$. It is particularly important to take this into account when considering the validity of the stability boundaries predicted by the two-mode time-averaged equations.

B. Two-Mode Continuation Results

In order to apply time-averaging, a sinusoidal time dependence is explicitly specified for each acoustic mode. This approximation is valid near the Hopf bifurcation point (i.e., for $\hat{\alpha}_1 \ll 1$), but as $\hat{\alpha}_1$ becomes larger the approximation becomes less valid. Continuation methods make it possible to compute the limit cycles of Eq. (4) as a function of one of the parameters of the system without resorting to time-averaging. Limit cycles of Eq. (4) exist as a result of the Hopf bifurcation that occurs at α_1 equal to zero. Figure 4 shows the results obtained by applying the continuation method to the two-mode approximation. The maximum amplitude of the pressure fluctuation at the head of the combustion chamber is used as a measure of the validity of the perturbation equations. Results in which the pressure perturbation is greater than one-half of the mean chamber pressure are probably not valid. The stability of the limit cycle is also indicated in Fig. 4; stable limit cycles are represented by solid lines, whereas unstable limit cycles are represented by dashed lines.

Results from the time-averaged equations are also plotted in Fig. 4 to show the differences between the continuation results and the results obtained by time-averaging. Results from the two methods are essentially the same for values of α_1 less than 120. Note that the change in the period of the limit cycle as a function of α_1 is poorly approximated by the time-averaged equations.

The limit cycle behaviors predicted by the continuation method and the time-averaged equations are significantly different for values of α_1 greater than 120. The continuation results show a turning point bifurcation at α_1 equal to 131, beyond which no limit cycle will exist. The limit cycle also

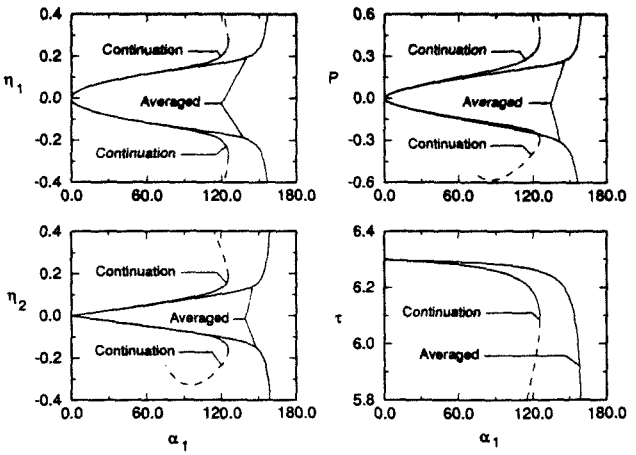

Fig. 4 Maximum amplitude of acoustic modes in limit cycle for two-mode approximation; —— stable, --- unstable.

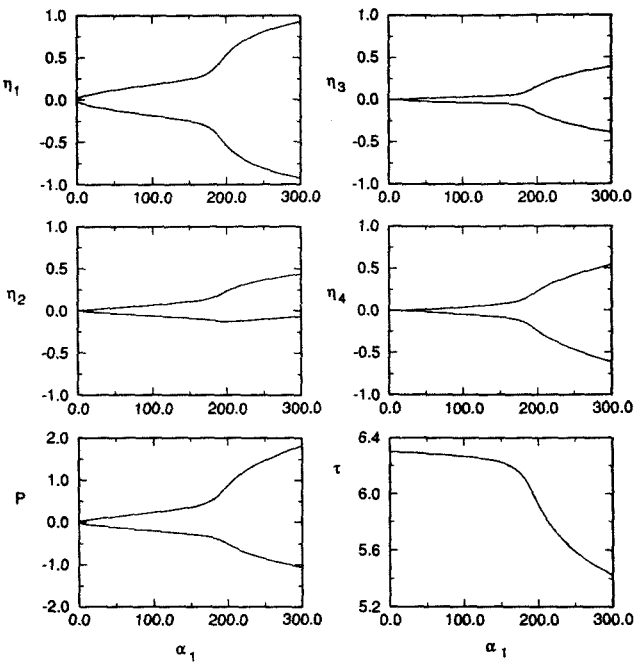

Fig. 5 Maximum amplitude of acoustic modes in limit cycle for four-mode approximation; —— stable, --- unstable.

becomes asymmetric near the turning point. This is particularly evident in the plot of the pressure fluctuation at the head of the combustion chamber. The limit cycle behavior predicted by the time-averaged equations remains symmetric by definition. Also note that the amplitude of the pressure perturbation at the turning point is close to one-half the mean chamber pressure so the perturbation expansion used to obtain the acoustic equations may not be valid.

C. Four-Mode Continuation Results

Figure 5 shows the limit cycle behavior of the four-mode approximation as a function of α_1. The results for the corresponding two-mode approximation are shown in Fig. 4. The most obvious difference between the two sets of results is that the stability boundary that occurred at the turning point in the two-mode approximation does not exist for the four-mode approximation.

In hindsight, it is not entirely surprising that the stability boundary determined by the two-mode approximation is sensitive to the number of acoustic modes included in the truncated system. The two-mode approximation, in which energy is produced by the linearly unstable first mode η_1, then transported to the stable second mode η_2, where it is subsequently dissipated is a gross approximation to the energy cascade that

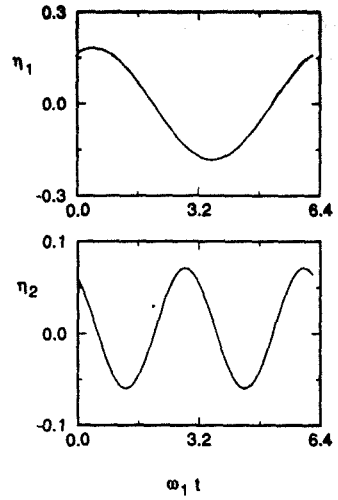

Fig. 6 Time-dependent amplitudes of acoustic modes in limit cycle obtained with continuation method for four-mode approximation, $\alpha_1 = 100$.

occurs in fluid dynamical systems. For slightly unstable systems (i.e., α_1 is small) the two-mode approximation is sufficient, as can be seen by comparing Figs. 4 and 5. For more unstable systems (larger values of α_1) it becomes difficult for the second mode to dissipate the energy produced by the first mode. At some point it becomes impossible for the second mode to dissipate all the energy produced by the first mode resulting in the turning point bifurcation, beyond which no limit cycles exist.

In the four-mode approximation, the third and fourth acoustic modes are also able to dissipate energy, resulting in a system that contains stable limit cycles for larger values of α_1. When α_1 is near 131, the value at which the turning point occurs in the two-mode approximation, the amplitudes of the third and fourth acoustic modes are about 10% of the mean chamber pressure. This is smaller than the amplitude of the second acoustic mode, but clearly significant to the energy balance in the limit cycle. Also note that the linear damping parameters of the higher-frequency modes are generally larger than the linear damping parameters of the lower-frequency modes (see Table 1). Therefore, as typical of fluid mechanical systems, higher frequency modes are more efficient at dissipating energy than lower frequency modes.

Figure 6 shows the time-dependent amplitudes of the first two acoustic modes for α_1 equal to 100. The amplitudes seem to have sinusoidal time dependence as was assumed in the time-averaging. It is interesting to note that the time-dependent amplitude of the second acoustic mode has a DC offset from 0. This seems to be the case for all values of α_1 with the offset increasing for increasing values of α_1. The maximum amplitude of the negative pressure fluctuation becomes larger than 1 when α_1 reaches 300, which is physically impossible. This underscores the importance of monitoring the amplitude of the pressure fluctuation to determine whether the results are physically realistic.

D. Six-Mode Continuation Results

In view of the major differences between the two- and four-mode approximations, it seems prudent to determine the limit cycle behavior of the six-mode approximation to determine whether or not there are differences between the limit cycle behavior of the four- and six-mode approximations. Figure 7 shows the maximum time-dependent amplitudes of the first two acoustic modes as functions of α_1 for the six-mode approximation. At first glance, the results for the six-mode approximation seem similar to the results for the four-mode approximation. A limit cycle exists and is stable for the entire range of values of α_1. On closer inspection however, one sees that the magnitudes of the time-dependent amplitudes are

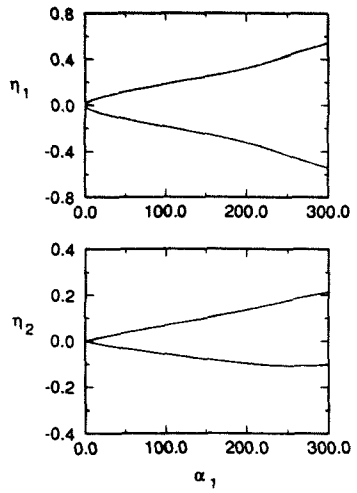

Fig. 7 Maximum amplitude of acoustic modes in limit cycle for six-mode approximation; —— stable, --- unstable.

smaller for the six-mode approximation than for the four-mode approximation for values of α_1 larger than 160.

This occurs because when more modes are included in the truncated system more modes are available to dissipate energy. When an insufficient number of modes are included in the approximation each mode must dissipate the amount of energy it naturally would, plus some of the energy that would be dissipated by higher-frequency modes. Thus, the required number of acoustic modes to include in the approximate system depends on the degree of instability of the system (i.e., the value of α_1). For larger values of α_1 it is necessary to include more modes in the approximation.

V. Results for a Second-Mode Instability

A. Two-Mode Approximation

The solution of the two-mode time-averaged equations is the same for a first- or second-mode instability, so the solution for the two-mode time-averaged system with an unstable second mode is given by Eq. (34). Stability boundaries for the two cases are different however. For the second-mode instability the solution is stable when[9]

$$\frac{(\beta^2 - 1) - \sqrt{(3\beta^2 + 1)(\beta^2 - 1)}}{(\beta^2 + 1)} < \frac{\alpha_2}{\alpha_1} < 0$$

For our system, where the only nonlinear terms are associated with second-order gasdynamic nonlinearities, the flow of energy is from low-frequency modes to high-frequency modes. In the present case the second mode is unstable, and so in the two-mode approximation energy is forced to flow from a higher frequency mode to a lower frequency mode. Thus, it is unlikely that the two-mode approximation is a valid model of the fluid mechanics when the second mode is unstable. The insufficiencies of the two-mode approximation can be seen more clearly by looking at the asymptotic expansion of the two-mode approximation. Using Eq. (4) it can be shown that the asymptotic solution of the two-mode approximation for $0 < \hat{\alpha}_2 \ll 1$ is

$$\begin{pmatrix} \eta_1 \\ \xi_1 \end{pmatrix} = \begin{pmatrix} 0 \\ 0 \end{pmatrix}$$

$$\begin{pmatrix} \eta_2 \\ \xi_2 \end{pmatrix} = e^{\hat{\alpha}_2 t} \begin{bmatrix} (1/\Omega_2)\sin \Omega_2 t + \cos\Omega_2 t \\ -\Omega_2 \sin \Omega_2 t + \cos \Omega_2 t \end{bmatrix} \qquad (35)$$

where

$$\Omega_2 = \sqrt{1 - \hat{\theta}_2 - (\hat{\alpha}_2/2)^2}$$

Only the second mode is linearly excited, as one would expect, because the acoustic modes are linearly uncoupled. Thus, if the second mode is to excite the first mode it must do so through the nonlinear terms. An examination of the two-mode approximation shows that the first mode is nonlinearly coupled to the second mode through the terms $\xi_1\xi_2$ and $\eta_1\eta_2$. With this form of coupling it is not possible for the second mode to excite the first mode if the first mode is initially unexcited.

Thus, modes of order greater than two must be included in the analysis of the second mode instability. Expanding Eq. (4) for a four-mode approximation one can show that nonlinear terms of the form η_2^2 and ξ_2^2 transfer energy from the second mode to the fourth mode when only the second mode is excited. Thus, the natural mode of energy transfer for the second-mode instability is from the unstable second mode to the stable fourth mode.

B. Four-Mode Time-Averaged Results

The four-mode time-averaged equations are determined with Eq. (6). An examination of the four-mode time-averaged equations shows that if the first, third, and fourth acoustic modes are initially unexcited while the second acoustic mode is excited, energy will be transported from the second mode to the fourth mode, but no energy will be transported from the second mode to either the first mode or the third mode. Further examination reveals that if the second and fourth modes are excited but the first and third modes are initially unexcited, then the first and third modes will remain unexcited for all time.

Since the odd acoustic modes can remain unexcited when the even acoustic modes are excited, one can look for steady states for which A_1, B_1, A_3, and B_3 are identically zero. The four-mode time-averaged system then reduces to a two-mode system that has the same form as the two-mode time-averaged system composed of the first and second acoustic modes. The solution of the time-averaged four-mode approximation is

$$\eta_1(t) = 0$$

$$\eta_2(t) = \frac{8\gamma}{(\gamma + 1)\omega_2} \sqrt{-\alpha_2\alpha_4(1 + \beta^2)}\sin[\omega_2 t + \phi_2(t)]$$

$$\eta_3(t) = 0$$

$$\eta_4(t) = \frac{8\gamma}{(\gamma + 1)\omega_2} \sqrt{\alpha_2^2(1 + \beta^2)}\sin[2\omega_2 t + \phi_4(t)] \qquad (36)$$

where

$$\phi_2(t) = -\left(\frac{\alpha_2\theta_4 + \alpha_4\theta_2}{2\alpha_2 + \alpha_4}\right) t + \phi_{20}$$

$$\phi_4(t) = -2\left(\frac{\alpha_2\theta_4 + \alpha_4\theta_2}{2\alpha_2 + \alpha_4}\right) t + \phi_{40}$$

$$\beta = \left(\frac{\theta_4 - 2\theta_2}{2\alpha_2 + \alpha_4}\right)$$

$$2\phi_{20} - \phi_{40} = \tan^{-1}(-\beta)$$

C. Four-Mode Continuation Results

Results for the four-mode approximation are obtained by expanding Eq. (4) and using the continuation method to determine the limit cycles of the resulting eighth-order system. A branch of limit cycles arises from the Hopf bifurcation point that occurs when α_2 is zero. Figure 8 shows the results of the continuation method along with the results from the time-averaged equations.

Figure 8 shows that the time-dependent amplitudes of the first and third modes are zero in the limit cycles predicted by

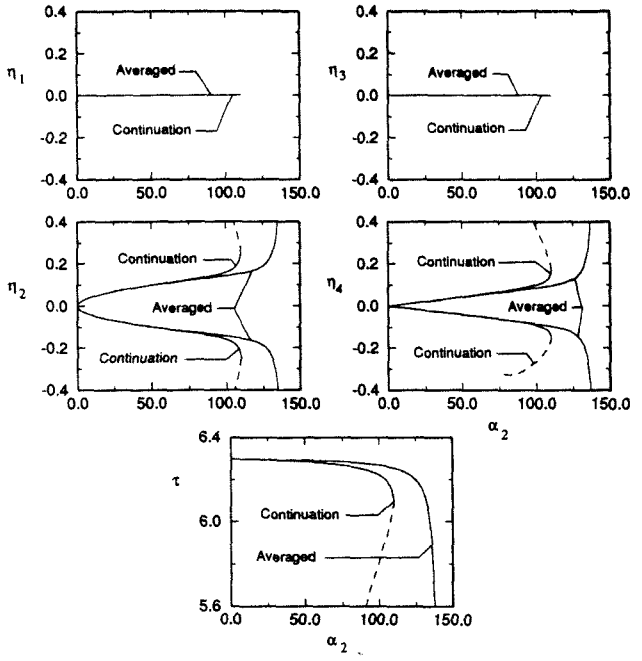

Fig. 8 Maximum amplitude of acoustic modes in limit cycle for four-mode approximation; —— stable, --- unstable.

the continuation method. This matches the solution of the time-averaged equations. The maximum amplitudes of the second and fourth acoustic modes in the limit cycle are essentially the same for the time-averaged and non-time-averaged systems when α_2 is less than 75. For values of α_2 larger than 75, the limit cycles predicted by the two methods start to diverge. The maximum amplitudes of η_2 and η_4 in the limit cycle predicted by the continuation method are larger than the maximum amplitudes of η_2 and η_4 predicted by time-averaging. Stability boundaries predicted by the two methods are substantially different. The stability boundary predicted by the continuation method occurs at α_2 equal to 109, whereas time-averaging predicts a stability boundary at α_2 equal to 140.

D. Six-Mode Continuation Results

Figure 9 shows the maximum amplitudes of the acoustic modes in the limit cycle as functions of α_2 for the six-mode approximation. For values of α_2 less than 84, the limit cycles for the four- and six-mode approximations are similar. The odd modes remain unexcited for both systems, whereas the even modes increase in amplitude as α_2 increases. For values of α_2 greater than 84, the limit cycles of the four- and six-mode approximation are qualitatively different. A pitchfork bifurcation of the limit cycles of the 6-mode approximation occurs at a value of α_2 of 84. This pitchfork bifurcation results in the formation of a stable branch of limit cycles on which the odd modes are excited. In the 4-mode approximation the odd modes remain unexcited for all values of α_2 studied. This should serve as a warning about making a priori assumptions about the solutions of nonlinear dynamical systems. If the odd modes had been assumed zero for all limit cycles in the six mode continuation results, the pitchfork bifurcation would not have been found.

As a result of the pitchfork bifurcation, two separate branches of limit cycles exist for values of α_2 greater than 84. On what will be called the primary branch, the odd modes have zero amplitude in the limit cycle. The limit cycles on this branch are stable up to the pitchfork bifurcation that occurs at α_2 equal to 84, and unstable for values of α_2 larger than 84. For the branch of limit cycles that occur as a result of the pitchfork bifurcation, here called the secondary branch, the odd modes have nonzero amplitudes. Since the odd modes are linearly stable, and thus able to dissipate energy when they have non-

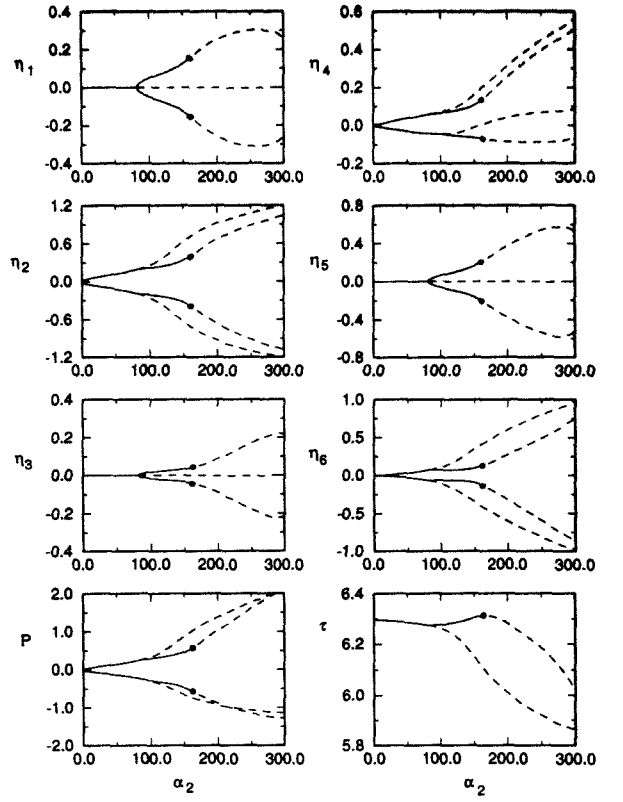

Fig. 9 Maximum amplitude of acoustic modes in limit cycle for six-mode approximation; —— stable, --- unstable, ●- Torus bifurcation.

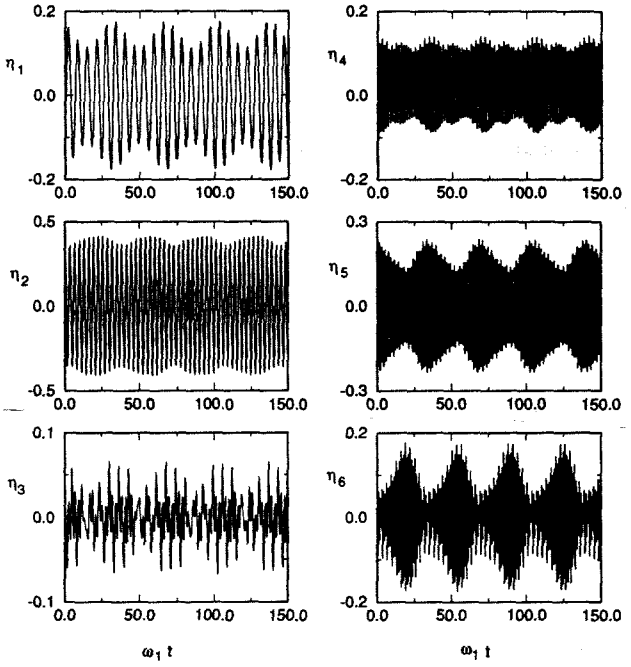

Fig. 10 Time simulation for six-mode approximation with $\alpha_2 = 160$.

zero amplitudes, the amplitudes of the even modes are smaller on the secondary branch than on the primary branch.

The secondary branch is linearly stable for values of α_2 from 84 to 155. A torus bifurcation occurs on the secondary branch at a value of α_2 of 155 causing the limit cycles to be unstable when α_2 is greater than 155. As a result of the torus bifurcation, a branch of toroidal solutions will appear for values of α_2 greater than 155. Figure 10 shows a time simulation for α_2 equal to 160. Multiple frequencies are clearly evident in the time simulation. The high-frequency content corresponds to the acoustic frequency of the combustion chamber, while the low-frequency content is a result of the torus bifurcation.

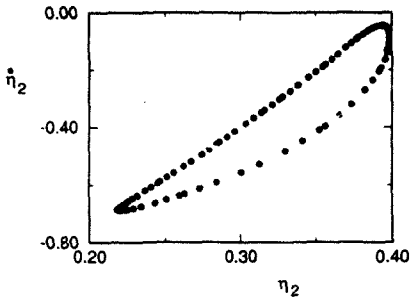

Fig. 11 Poincare map of the time simulation of the six-mode approximation with $\alpha_2 = 160$.

It is difficult to assign any physical meaning to the low-frequency oscillations as the toroidal motion is highly nonlinear. Figure 11 shows a Poincare map of the time simulation of Fig. 10. The closed orbit in Fig. 11 clearly shows that the motion is toroidal for α_2 equal to 160.

VI. Conclusions

One major result of this analysis has been to show that for a first-mode instability the stability boundaries predicted with the two-mode time-averaged equations are artifacts of the two-mode approximation. A stability boundary is also found when the continuation technique is used to calculate the limit cycles of the two-mode nontime-averaged equations, so the existence of the stability boundary is characteristic of the two-mode approximation and is not the result of time-averaging.

No stability boundary is found for the four- or six-mode continuation results for the case of an unstable first mode. A limit cycle exists and is stable for all values of α_1 examined in this study. There is a significant difference in the magnitude of the time-dependent amplitudes of the acoustic modes in the limit cycles for the four- and six-mode approximations for large values of α_1. In the neighborhood of the Hopf bifurcation point ($\alpha_1 = 0$) the results of the various approximations are almost identical and they remain relatively close for values of α_1 less than 100. Results for the four- and six-mode approximations diverge rapidly as α_1 becomes larger than 160 as more modes are necessary to dissipate the additional energy produced by the more unstable first mode.

In the case of the second-mode instability, it has been found that the two-mode approximation consisting of the first and second acoustic modes does not allow for the natural transfer of energy from low-frequency to high-frequency modes, and it is not possible for the second mode to excite the first mode if the first mode is initially unexcited. An examination of the equations representing the time evolution of the time-dependent amplitudes of the acoustic modes shows that when the second acoustic mode is unstable, nonlinear energy transfer will occur from the unstable second mode to the stable fourth mode. There is no mechanism for the second or fourth acoustic modes to excite the first and third acoustic modes if the first and third acoustic modes are initially unexcited.

Results for the six-mode approximation with a second-mode instability predict limit cycle behavior not seen before. A pitchfork bifurcation of the primary branch occurs for α_2 equal to 84 and results in a new branch of limit cycles that have odd modes with nonzero amplitudes in the limit cycle. Thus, for α_2 greater than 84 it is possible for energy to flow from the even modes to the odd modes. This new branch of limit cycles contains a torus bifurcation resulting in quasiperiodic motions. Similar to the case of the first-mode instability, the number of modes required in an analysis of the second-mode instability depends on the degree of instability of the system.

References

[1]Crocco, L., and Chang, S.-I., "Theory of Combustion Instability in Liquid-Propellant Rocket Motors," AGARDograph No. 8, Butterworth's Scientific Publications, London, 1956.

[2]Mitchell, C. E., Crocco, L., and Sirignano, W. A., "Nonlinear Longitudinal Instability in Rocket Motors with Concentrated Combustion," *Combustion Science and Technology*, Vol. 1, 1969, pp. 35–63.

[3]Zinn, B. T., and Savell, C. T., "A Theoretical Study of Three-Dimensional Combustion Instability in Liquid-Propellant Rocket Engines," *Proceedings of the Twelfth International Symposium on Combustion*, Williams and Wilkins Co., Baltimore, MD, 1969, pp. 139–147.

[4]Zinn, B. T., and Powell, E. A., "Application of the Galerkin Method in the Solution of Combustion-Instability Problems," Vol. 3, *Propulsion Re-Entry Physics*, Pergamon, Oxford, England, UK, 1970.

[5]Culick, F. E. C., "Nonlinear Growth and Limiting Amplitude of Acoustic Oscillations in Combustion Chambers," *Combustion Science and Technology*, Vol. 3, No. 1, 1971, pp. 1–16.

[6]Culick, F. E. C., "Nonlinear Behavior of Acoustic Waves in Combustion Chambers—I," *Acta Astronautica*, Vol. 3, 1976, pp. 715–734.

[7]Culick, F. E. C., "Nonlinear Behavior of Acoustic Waves in Combustion Chambers—II," *Acta Astronautica*, Vol. 3, 1976, pp. 735–757.

[8]Culick, F. E. C., and Levine, J. N., "Comparison of Approximate and Numerical Analysis of Nonlinear Combustion Instabilities," AIAA Paper 74-201, 1974.

[9]Paparizos, L., and Culick, F. E. C., "The Two-Mode Approximation to Nonlinear Acoustics in Combustion Chambers I. Exact Solutions for Second Order Acoustics," *Combustion Science and Technology*, Vol. 65, 1989, pp. 39–65.

[10]Guckenheimer, J., and Holmes, P., *Nonlinear Oscillations, Dynamical Systems, and Bifurcations of Vector Fields*, Springer-Verlag, New York, 1980.

[11]Ioos, G., and Joseph, D., *Elementary Stability and Bifurcation Theory*, Springer-Verlag, New York, 1980.

[12]Doedel, E., and Kernevez, J., "Software for Continuation Problems in Ordinary Differential Equations with Applications," Preprint, CALTECH, Pasadena, CA, 1984.

[13]Keller, H. B., "Numerical Solution of Bifurcation and Nonlinear Eigenvalue Problems," *Applications of Bifurcation Theory*, Academic Press, New York, 1977.

[14]Press, W. H., Flannery, B. P., Teukolsky, S. A., and Vetterling, W. T., *Numerical Recipes—The Art of Scientific Computing*, Cambridge Univ. Press, 1989.

[15]Jahnke, C. C., "Analysis of the Second Order Nonlinear Acoustic Equations with Two Modes," CALTECH, Guggenheim Jet Propulsion Center Documents on Active Control of Combustion Instabilities, Document No. CI90-1, Pasadena, CA, 1990.